analytical chemistry

Article

pubs.acs.org/ac

Highly Sensitive Photoelectrochemical Immunoassay with Enhanced Amplification Using Horseradish Peroxidase Induced Biocatalytic Precipitation on a CdS Quantum Dots Multilayer Electrode

Wei-Wei Zhao, Zheng-Yuan Ma, Pei-Pei Yu, Xiao-Ya Dong, Jing-Juan Xu,* and Hong-Yuan Chen

State Key Laboratory of Analytical Chemistry for Life Science, School of Chemistry and Chemical Engineering, Nanjing University, Nanjing 210093, China

Supporting Information

ABSTRACT: Herein we demonstrate the protocol of a biocatalytic precipitation (BCP)-based sandwich photoelectrochemical (PEC) horseradish peroxidase (HRP)-linked immunoassay on the basis of their synergy effect for the ultrasensitive detection of mouse IgG (antigen, Ag) as a model protein. The hybrid film consisting of oppositely charged polyelectrolytes and CdS quantum dots (QDs) is developed by the classic layer by layer (LbL) method and then employed as the photoactive antibody (Ab) immobilization matrix for the subsequent sandwich-type Ab-Ag affinity interactions. Improved sensitivity is achieved through using the bioconjugates of HRP-secondary antibodies (Ab_2). In addition to the much enhanced steric hindrance compared with the original one, the presence of HRP would further stimulate the BCP onto the electrode surface for signal amplification, concomitant to a competitive nonproductive absorption that lowers the photocurrent intensity. As a result of the multisignal amplification in this HRP catalyzed BCP-based PEC immunoassay, it possesses excellent analytical performance. The antigen could be detected from 0.5 pg/mL to 5.0 ng/mL with a detection limit of 0.5 pg/mL.

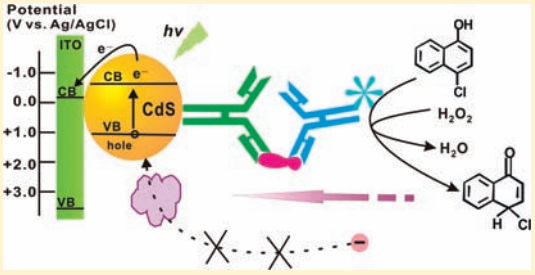

Immunoassays have attracted substantial interest with the expectation of obtaining prompt, accurate, and sensitive immunological response for food safety, environmental monitoring, and medical and clinical diagnosis.[1] The conventional immunoassays involving radioimmunoassay[2] and enzyme-linked immunoassay,[3] which are subsequently coupled to various techniques such as piezoelectricity,[4] surface plasmon resonance,[5] electrochemistry,[6] and electrochemiluminescence (ECL)[7] with the aim to exploit and develop improved immunoassays. Among them, electrochemical immunoassay has gained tremendous research efforts because of the low detection limit and high selectivity for analyzing complex samples that could be achieved cost-effectively with relatively simple instrumentation. Although previous works have demonstrated electrochemical detection in conjunction with many assay formats, the sandwich enzyme immunoassay (EIA) is especially popular for its capability of signal enhancement.[8,9]

The photoelectrochemical (PEC) detection is a newly appeared yet dynamically developing technique for biological sensing. Essentially, like other well established technique such as ECL, the PEC method is also evolved from the electrochemistry. However, it is different from the traditional electrochemical methods greatly and offers some merits that could not be realized on the latter. In PEC detection, light is utilized to excite the photoactive species and current is employed as the detection signal. Because of this total separation and the different energy form of the excitation source and detection signal, this technique possesses potentially higher sensitivity than the conventional electrochemical methods because of the reduced background signals.[10] Its sensing principle is that photocurrent variation could be brought about by the biological interactions between various recognition elements and their corresponding target analytes.[11−15] On the other hand, advantageously inherited from the electrochemical technique, the use of an electronic readout makes the instrument simpler, cheaper, and easier to miniaturize than that of conventional optical methods.[16,17] Given the advantages mentioned above, it is surprising that not much work has been done in this area, especially in its exploitation for the immunoassay. Specifically, only rather limited works addressing the determination of anticholera toxin Ab,[18,19] α-fetoprotein,[20] mouse IgG,[21] and pentachlorophenol[22] have been reported in the past decade. In these investigations, the label-free method, which is based on the direct Ab-Ag affinity without markers, has been chosen for the purpose of saving time and cost.[18−22] Despite the good simplicity, the analytical performances of these PEC label-free protocols still need to be improved due to the low capacity of analyte loading and inability for amplification. Hence, on the basis of combining the enzyme-labeled immunoassay with the PEC technique, development of an enzyme-labeled sandwich PEC immunoassay might be a useful route for signal enhancement. Recently, the glucose oxidase (GOx) labeled PEC immunoassay was exploited by Zhang and co-workers for the detection

Received: July 16, 2011
Accepted: December 12, 2011
Published: December 12, 2011

Scheme 1. Development of the Amplified QD-Based Sandwich PEC Immunoassay with HRP-Catalyzed BCP Format

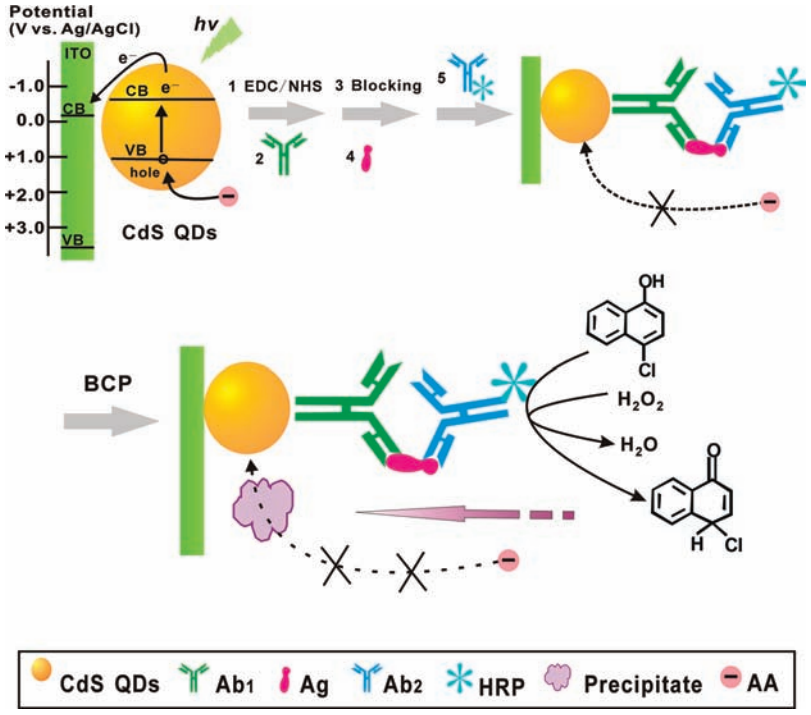

of α-Synuclein based on the production of electron donor H_2O_2 by the labeled GOx.[23] However, since its design was relying on that the immunocomplex was formed on one side whereas the detection signal was generated on the another side of the electrode, the introduced GOx labels just acted as the enzyme to catalyze its substrate for H_2O_2 production. Regretfully, signal amplification could not be achieved in that assay format, and hence its analytical performance was only close to previous label-free strategies. Until now, the amplified PEC immunoassay is still highly expected and has not yet been reported as far as we know; thus, the realization of a new PEC immunoassay with enhanced amplification would obviously be desirable.

Enzymatic biocatalytic precipitation (BCP), involving the formation of insoluble products on the electrode surface, has been utilized for extending the detection limits via mass amplification in the analytical fields.[24,25] For the application of BCP in PEC detection, our earlier report has demonstrated that the buildup of an insulating layer on the electrode could alter the interfacial electron-transfer feature greatly, i.e., the extremely tiny perturbation of the interface property could significantly influence the photocurrent due to the introduced barrier for the interfacial holes arrested by the electron donor.[26] If BCP is integrated into the enzyme-labeled PEC immunoassay, one can expect that the presence of the Ab_2-enzyme bioconjugates could not only lead to the formation of an insulating barrier but also enhance the original steric hindrances, suggesting that the signal could be amplified greatly. In addition, since many enzyme labels (e.g., horseradish peroxidase, HRP) usually possess strong light-harvesting properties at certain wavelengths, the properly selected enzyme could simultaneously exhibit a competitive nonproductive absorption that lowers the photocurrent intensity for greater signal amplification. The possibility of multisignal amplification should be attributed to the synergy effect between PEC detection and enzyme catalyzed BCP. However, this type of amplified PEC immunoassay with anticipated better performance has never been exploited.

Since their discovery, QDs have attracted substantial research efforts and emerged as a significant new class of materials with great potential in different optoelectronic applications due to their unique features: nanoscale size similar to proteins, broad excitation spectra, and versatility in surface modification.[27] While QDs have found their wide utilization in a plethora of ultrasensitive optical, electrochemical, or electrochemiluminescent bioassays,[28−30] rather limited effort is exerted on their application in PEC detection[14,19,31] and the potential in this field still needs to be exploited.

In present work, we report the first QDs-based amplified PEC immunoassay with the integration of HRP catalyzed BCP for multiamplification with the aim to search for an advanced immunoassay format. Experimentally, the Ab_1 was initially anchored onto the CdS QDs modified indium tin oxide (ITO) electrode for the subsequent immunorecognition between Ab_1 and analyte Ag, followed by the labeling of HRP via Ab_2 ($HRP-Ab_2$ bioconjugates) for the final introduction of BCP into the PEC detection system, on the basis of HRP accelerated oxidation of 4-chloro-1-naphthol (4-CN) by H_2O_2 to yield the insoluble and insulating product benzo-4-chlorohexadienone on the transducer surface, Scheme 1. Besides, the competitive light absorption of HRP would meanwhile lower the irradiation intensity on the transducer and thus inhibit the photocurrent generation. Because of the synergy effect of their coupling, this present amplified PEC immunoassay, as compared to those previously established PEC immunoassays, has inherent higher sensitivity for the detection of mouse IgG as a model protein in clinical diagnosis and to the best of our knowledge has never been reported. The detailed preparation, characterization, and desirable performance characteristics of the developed amplified PEC immunoassay are described in the following section.

dx.doi.org/10.1021/ac203184g | *Anal. Chem.* 2012, 84, 917−923

EXPERIMENTAL SECTION

Reagents. The ITO slices (type N-STN-S1-10, China Southern Glass Holding Co., Ltd.) were used as the working electrode. Mouse IgG (Ag), polyclonal goat antimouse IgG (Ab_1) and HRP-labeled polyclonal goat antimouse IgG (Ab_2) were obtained from Boster Biological Technology, Ltd. (Wuhan, China). *N*-(3-Dimethylaminopropyl)-*N*-ethyl-carbodiimide hydrochloride (EDC), *N*-hydroxysuccinimide (NHS), poly(diallyldimethylammonium chloride) (PDDA; 20%, w/w in water, MW = 200 000−350 000), bovine serum albumin (BSA), and thioglycolic acid (TGA) were purchased from Sigma-Aldrich (St. Louis, MO). Tween 20 was purchased from Amresco. 4-Chloro-1-naphthol (4-CN) was obtained from Tokyo Kasei Kogyo Co., Ltd. (Japan). Ascorbic acid (AA) was obtained from Sinopharm Chemical Reagent Co., Ltd. (China). Other chemicals were of analytical reagent grade and used as received. PBS (0.01 M, pH 7.4) was used for the preparation of the Ag and Ab solutions. The washing buffer solution was 0.01 M PBS (pH 7.4) containing 0.05% Tween 20. The blocking buffer was 0.01 M PBS (pH 7.4) containing 3% (w/v) BSA. All aqueous solutions were prepared using ultrapure water (Milli-Q, Millipore).

Apparatus. PEC measurements were performed with a homemade PEC system equipped with a 500 W Xe lamp and a monochromator. Photocurrent was measured on a CHI 750a electrochemical workstation (China) with a three-electrode system: a modified ITO electrode with a geometrical area of 0.25 ± 0.01 cm^2 as the working electrode, a Pt wire as the counter electrode, and a saturated Ag/AgCl electrode as the reference electrode. All the photocurrent measurements were performed at a constant potential of 0 V (versus Ag/AgCl). A 0.1 M PBS containing 0.1 M AA was used as the blank solution for photocurrent measurements, which was degassed by highly pure nitrogen for 15 min before PEC experiments and then kept over a N_2 atmosphere for the entire experimental process. Electrochemical impedance spectroscopy (EIS) was carried out with an Autolab potentiostat/galvanostat (PGSTAT 30, Eco Chemie B.V., Utrecht, The Netherlands) and controlled by FRA 4.9 software with a three-electrode system, the same as in the PEC detection in 0.1 M KCl containing a 5.0 mM $K_3[Fe(CN)_6]/K_4[Fe(CN)_6]$ (1:1) mixture as a redox probe. Transmission electron microscopy (TEM) was performed with a JEOL model 2000 instrument operating at 200 kV accelerating voltage. The UV−vis absorption spectra were obtained on a Shimadzu UV-3600 UV−vis-NIR photospectrometer (Shimadzu Co.). The ζ-potential was acquired with a Malvern (Nano-Z) instrument. Atomic force microscopy (AFM) images were performed in ambient conditions using a molecular imaging Pico SPM in tapping mode with a 10 μm scanner.

Synthesis of TGA-Stabilized CdS QDs and the Fabrication of Electrode. The utilized CdS QDs was synthesized according to the previous report with a slight modification.[21] Briefly, 250 μL of TGA was added to 50 mL of 1.0×10^{-2} M $CdCl_2$ aqueous solution, and N_2 was bubbled throughout the solution to remove O_2 for 30 min at 110 °C. During this period, 1.0 M NaOH was added to adjust the above solution to the desired value of pH 11. Then, 5.5 mL of 0.1 M Na_2S aqueous solution was injected into this solution to obtain TGA-capped water-soluble CdS QDs, and the reaction mixture was refluxed under N_2 atmosphere for 4 h. This procedure produced CdS QDs with a Cd to S (Cd/S) ratio of 1:1.1. Finally, the desired TGA-stabilized CdS QDs were obtained and then diluted with the same volume of water and stored in a refrigerator at 4 °C for further use. The PDDA/CdS multilayer film was grown by alternately dipping of the freshly cleaned ITO slices into a solution of 2% PDDA containing 0.5 M NaCl and the as-obtained CdS QDs solution for 10 min, respectively, and this process was repeated three times to obtain desired photocurrent intensity. The films were carefully washed with doubly distilled water after each dipping step.

Immunoassay Development. Ab_1 was immobilized onto the CdS QDs modified ITO electrode via the classic EDC coupling reactions between COOH groups on the surface of the TGA-capped CdS QDs and the NH_2 groups of the Ab. In detail, the CdS QDs modified electrode was activated by immersion in 1.0 mL of distilled water containing 20 mg of EDC and 10 mg of NHS for 1 h at room temperature, followed by thoroughly rinsing with washing buffer to wash off the excess EDC and NHS. Subsequently, 25 μL of 0.5 mg/mL Ab_1 was spread onto the resulting electrode surface at 4 °C in a moisture atmosphere to avoid evaporation of solvent. After incubation for 16 h, the electrode was rinsed with the washing buffer to remove physically absorbed Ab_1. The electrodes were then blocked with 25 μL of blocking solution for 2 h at 4 °C to block nonspecific binding sites and washed with the washing buffer thoroughly. Next, 25 μL of analyte Ag with different concentrations was dropped onto the Ab_1 modified electrodes for an incubation of 60 min at 37 °C followed by washing with washing buffer. After the binding reaction between Ab_1 and Ag, the electrodes were allowed for labeling by additional incubation with 25 μL of diluted Ab_2-HRP bioconjugates solution for 60 min, and again the electrodes were washed thoroughly with water to remove nonspecifically bound conjugations, which could cause a background response before measurement. To prepare the BCP solution, 4-CN was first dissolved in ethanol and then the ethanolic stock solution was diluted with 0.1 M PBS, pH 7.4, to compose the solution that includes 1×10^{-3} M 4-CN and 2% (v/v) ethanol. Finally, the Ab_1-Ag-Ab_2-HRP modified electrodes were allowed for 10 min incubation at 25 °C in the obtained BCP solution consisting of 1×10^{-3} M 4-CN and 1.5×10^{-4} M H_2O_2. After incubation of the respective electrodes in the BCP solution, the electrodes were rinsed with 0.01 M phosphate buffer, pH 7.4, and then introduced to the respective PEC measurements.

RESULTS AND DISCUSSION

Characterization of CdS QDs Modified ITO Electrode. The TEM imaging and the UV−vis absorption were used to characterize the prepared CdS QDs with the results shown in Figures S-1 and S-2 in the Supporting Information. The LbL assembly of oppositely charged polyelectrolytes and nanoparticles has been widely studied as an effective route to fabricate multifunctional hybrid materials.[32] The surface of the ITO electrode was coated with a large number of hydroxyl groups. The ζ-potential of the utilized cationic polyelectrolyte PDDA and TGA-capped CdS QDs were determined to be +6.27 mV and −16.6 mV, respectively. Experimentally, the negatively charged ITO electrode was electrostatically attracted to the PDDA, which would offer a homogeneous distribution of positive charges for the following efficient anchoring of negatively charged CdS QDs onto the electrode surface by means of electrostatic adsorption. As shown in Figure S-3 in the Supporting Information, the photocurrent action spectra of the as-obtained electrode overlapped the absorbance spectrum of

dx.doi.org/10.1021/ac203184g | *Anal. Chem.* 2012, 84, 917−923

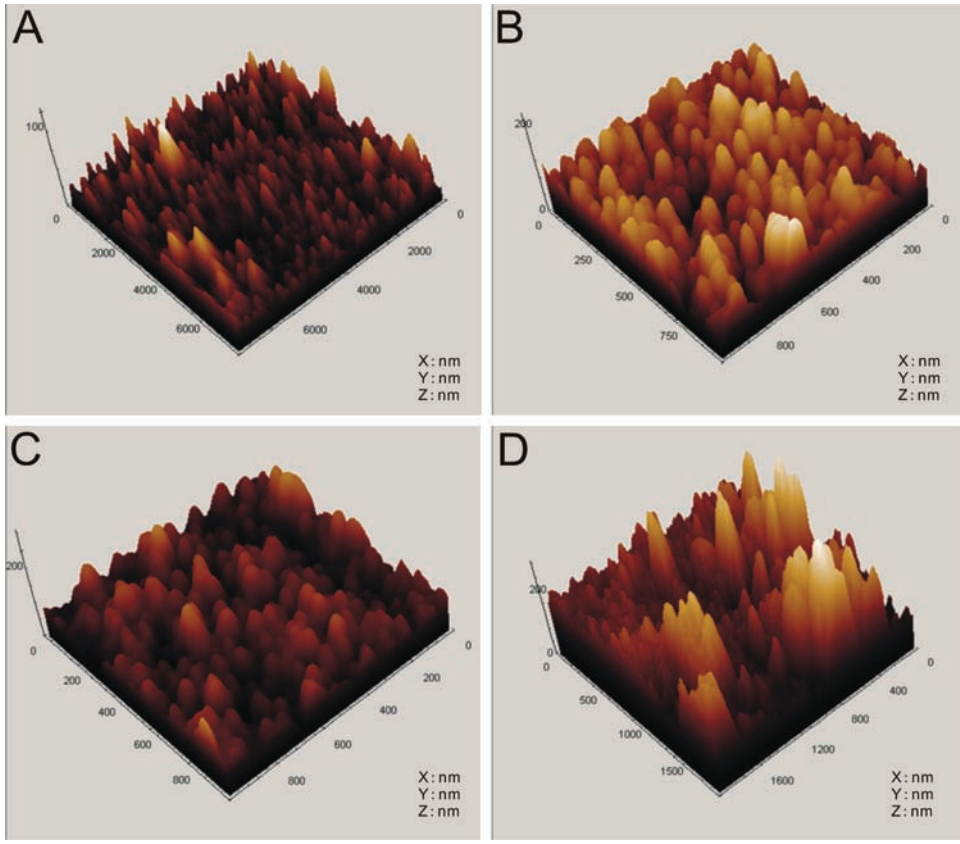

Figure 1. AFM images of (A) bare CdS QDs modified electrode ; (B) after Ab_1 immobilization; (C) after the BSA blocking, the Ag anchoring corresponding to 5.0×10^{-6} g/mL and further HRP-Ab_2 labeling corresponding to 5.0×10^{-6} g/mL; and (D) after the final 10 min HRP induced BCP.

the CdS QDs, implying the CdS QDs had been successfully assembled onto the electrode. Figure S-4 in the Supporting Information shows the operational stability of the electrode, which indicated that the fabricated electrode had high mechanical and photophysical stability in the AA solution and was suited for application in the PEC immunoassay.

Characterization of the Immunoassay Development Process. *AFM Measurement.* The surface topography and phase images of the immunoassay development process were recorded by AFM imaging as shown in Figure 1. Figure 1A presents the image of the rough electrode surface after the electrostatic binding of the CdS QDs. Evidently, the surface coverage of CdS QDs was substantially high with a complete and nearly homogeneous CdS QDs layer formed on the ITO surface in large scale (with an area of 8000 nm × 8000 nm shown). The rough surface with highly specific surface area would be advantageous for loading more protein molecules. Figure 1B reveals the AFM image of the electrode surface after the covalent immobilization of Ab_1 on the CdS QDs layer. Obviously, the difference between parts A and B of Figure 1 indicates the presence of an anchored Ab_1 layer, and a few aggregates of the Ab_1 could still be observed on the surface even though the Ab_1-modified surface was thoroughly rinsed. Figure 1C demonstrates the AFM image of the electrode surface after the labeling of HRP-Ab_2. Making a comparison between panels in parts B and C of Figure 1, it was found that the surface morphology of Figure 1C was more compact and some large aggregates of biomolecules could be observed, which should be attributed to the blocking of BSA filling the interstitial places and forming of a sandwich immunocomplex from the specific immunoreaction, respectively. The distinctive difference in the topography with the enhanced roughness of Figure 1D indicates the successful BCP on the electrode surface.

EIS Measurement. As an effective tool for characterizing the interface properties of electrodes, EIS was also utilized to monitor the fabrication process. As shown in Figure 2, for the

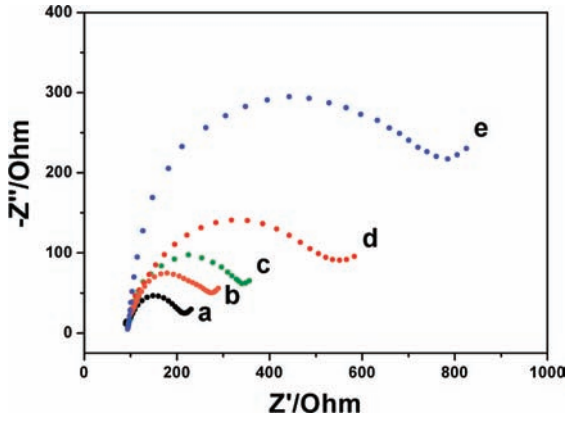

Figure 2. EIS of (a) bare CdS QDs modified electrode electrodes, (b) after Ab_1 immobilization, (c) after anchoring the Ag corresponding to 5.0×10^{-6} g/mL, (d) after further labeling of HRP-Ab_2 corresponding to 5.0×10^{-6} g/mL, and (e) after final 10 min HRP induced BCP. The EIS measurements are carried out in 0.1 M KCl containing 5.0 mM $K_3Fe(CN)_6/K_4Fe(CN)_6$ (1:1). The frequency range was between 0.01 and 100 000 Hz with an applied voltage of 5 mV.

dx.doi.org/10.1021/ac203184g | *Anal. Chem.* 2012, 84, 917–923

bare CdS QDs electrode, the impedance spectrum exhibited a small semicircle (curve a). Comparing curves a and b, one can see that after the Ab_1 is covalently immobilized on the electrode surface, the resistance R_{et} increases obviously. After the BSA blocking and subsequent stepwise immobilization of Ag, HRP-Ab_2 bioconjugates, and BCP, the R_{et} increases gradually as the experiment proceeds (curves c–e), turning out the successful assembling of sensing and amplifying elements and the BCP on the electrode surface. The reason for the resistance increase is that the nonconductive properties of the proteins and the insoluble precipitation layer progressively obstruct the mass transport and electron transfer of the electrochemical probe to the electrode surface by elevating the hindrance effect and final insulating effect.

Amplified PEC Immunoassay Based on HRP Induced BCP. As shown in Figure 3, the immunoassay development process was monitored by PEC measurement progressively. After anchoring the Ab_1 and blocking by BSA on the CdS QDs modified electrode, the photocurrent decreased (curves b and c). This could be easily attributed to the generated steric hindrances that the immobilization of the proteins on the modified electrode generated a hydrophobic layer and thus partly hindered the diffusion of AA to the surface of CdS QDs for reaction with the photogenerated holes. After the as-produced electrode was further incubated with the analyte Ag and the HRP-Ab_2 bioconjugates, the photocurrent maintained only ~53% and 37% of the initial intensity (curves d and e), respectively. After the as-obtained electrode was incubated with the corresponding BCP solution, the photocurrent intensity further decreased prominently to ~20% of the initial intensity (curve f). Whereas the exclusive cause of photocurrent variation prior to and after the biorecognition event had been attributed to the enhanced steric hindrances toward the diffusion of quencher molecules in those label-free PEC immunoassays[18−22] or to the enhanced donor concentration in the GOx-labeled PEC immunoassay,[23] in this proposed amplified PEC immunoassay there are at least three possible reasons for the photocurrent reduction: (1) The donor diffusion rate is intimately dependent on the interfacial property of the electrode. So from the traditional perspective of steric hindrance, the formation of Ab_1-Ag-Ab_2-HRP sandwich immunocomplexes via the introduction of HRP-Ab_2 bioconjugates, as compared with Ab_1-Ag alone, would greatly increase the steric hindrance and hence retard the diffusion of donor molecules to the surface of the underlying CdS QDs film; the reduced interfacial donor concentration would subsequently inhibit the efficiency of hole scavenging and thus enhance undesired recombination, leading to the photocurrent decrease. (2) The formation of insoluble and insulating product by BCP would thereby introduce an isolating barrier for the electron-transfer at the electrode interface and alter the light-absorption feature of the electrode greatly. As a result, the holes of the excited CdS QDs cannot interact with the donor directly due to the direct blocking by the precipitate, which could diminish the hole trapping capacity of CdS QDs and hence lead to the inefficient generation of photocurrent. (3) HRP, which is usually conjugated to an Ab in a 4:1 ratio, has been widely used as secondary detection reagents in an enzyme-linked immunosorbent assay (ELISA). However, in the present PEC immunoassay, HRP is not just a label to induce BCP but can meanwhile act as a competitor of light absorption at 410 nm due to the strong light-harvesting property of HRP at around 380–420 nm,[33] which would also result in a competitive nonproductive absorption that lowers the photocurrent intensity.[26] Previous work has also observed the presence of

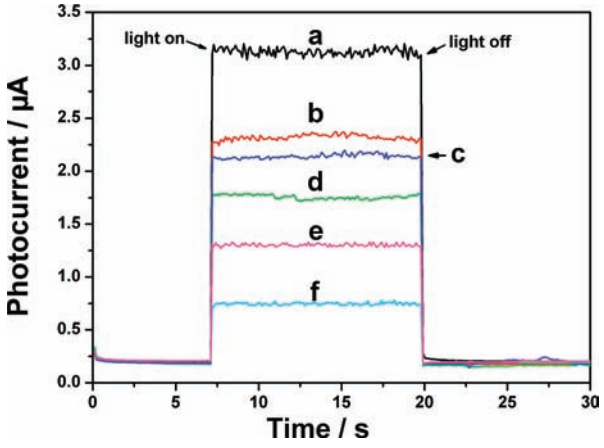

Figure 3. Photocurrent response of CdS QDs modified electrode electrodes (a) before and (b) after Ab_1 immobilization, (c) after further blocking with BSA, (d) after anchoring the Ag corresponding to 5.0×10^{-6} g/mL, (e) after further labeling of HRP-Ab_2 corresponding to 5.0×10^{-6} g/mL, and (f) after a final 10 min enzyme catalyzed BCP. The PEC tests were performed in 0.1 M PBS containing 0.1 M AA with 0 V applied potential and 410 nm excitation light.

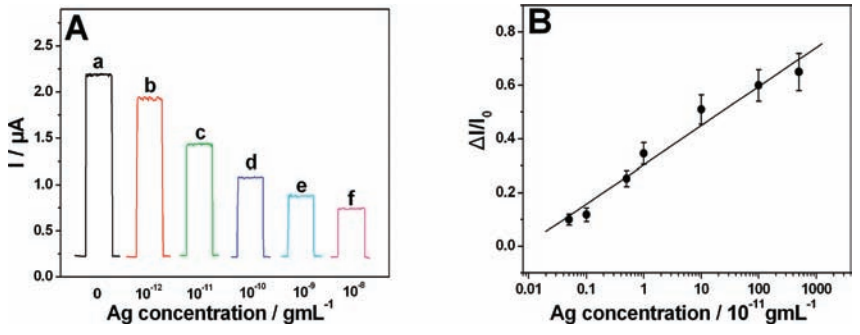

Figure 4. (A) Effect of different concentrations of Ag on the differential photocurrent responses. (B) The corresponding calibration curve. $\Delta I = I_0 - I$, I_0 was the photocurrent of the modified electrode prior to Ag immobilization and I was the final photocurrent of the electrode after incubation with Ag of elevated concentrations corresponding to (a) 0, (b) 10^{-12}, (c) 10^{-11}, (d) 10^{-10}, (e) 10^{-9}, and (f) 10^{-8} g/mL, respectively, and then after the final BCP. The photocurrent responses were measured in 0.1 M PBS containing 0.1 M AA with an applied potential of 0 V and light wavelength of 410 nm.

dx.doi.org/10.1021/ac203184g | Anal. Chem. 2012, 84, 917–923

Table 1. Analytical Performance of Various Mouse IgG Immunoassays and the Recently Reported PEC Immunoassays

analyte	measurement protocol	linear range	detection limit	ref
mouse IgG	standard ELISA kit	9.375−600 ng/mL	9.375 ng/mL	35
mouse IgG	electrochemical immunoassay	0.01−250 ng/mL	6.1 pg/mL	36
mouse IgG	fluoroimmunoassay	0−10 μg/L	57 pg/mL	37
mouse IgG	surface plasmon resonance immunoassay	≤100 ng/mL		38
mouse IgG	chemiluminescent immunoassay	250−2500 ng/mL	25 ng/mL	39
mouse IgG	label-free PEC detection	10 pg/mL to 100 ng/mL	8 pg/mL	21
anticholera toxin Ab	label-free PEC detection		0.5 μg/mL	19
α-fetoprotein	label-free PEC detection	50 pg/mL to 50 ng/mL	40 pg/mL	20
pentachlorophenol	label-free PEC detection	1 nM to 0.3 μM	1 pM	22
α-synuclein	GOx-labeled PEC detection	50 pg/mL to 100 ng/mL	34 pg/mL	23
mouse IgG	amplified HRP-labeled PEC detection	0.5 pg/mL to 5.0 ng/mL	0.5 pg/mL	

the strong absorption effect of HRP could affect the photocurrent response of TiO_2 nanotube electrodes.[34] Control experiments, which were performed with the Ab_1 modified photoelectrode incubated in PBS solution without Ag at 37 °C for 60 min and then in the BCP solution, manifested no change in the photocurrent intensity, further implying that the photocurrent reduction was due to the immunoreaction and labeling.

Optimization of Experimental Conditions. In addition to the PEC measurement conditions, several parameters including incubation temperature and time, HRP-Ab_2 concentration, and the BCP time were also very crucial to achieve the optimal immunoassay performance. So we studied these factors, and 37 °C of incubation temperature, 60 min of incubation time, 1.5×10^{-6} g/mL of Ab_2-HRP concentration, and a BCP time of 10 min were chosen for the following experiments. The detailed investigations and discussion are in the Supporting Information with the results shown in Figures S-5−S-8 in the Supporting Information.

Calibration Curve of the Developed Immunoassay. The degree of signal variation in this amplified PEC immunoassay is directly related to the concentration of target Ag. Hence, by tracking the transduction signal that monitors the amount of immunocomponents, a new immunoassay can be accomplished. Figure 4A presents the photocurrents after incubation with Ag of variable concentrations. The photocurrent decreases with the increase of the concentration of Ag. As shown in Figure 4B, the percentage of the photocurrent decrement was proportional to the logarithm of the Ag concentrations in a linear range from 0.5 pg/mL to 5.0 ng/mL. Upon the treatment of the sensing interface with increasing Ag concentration, more sandwich immunocomplexes could be induced and more precipitate would deposit onto the electrode interface; over 5.0 ng/mL the reduction was prone to saturation. The detection limit was experimentally found to be 0.5 pg/mL. In addition, we further compared this proposed PEC immunoassay not only with other mouse IgG immunoassays but also with all the previously reported PEC immunoassay protocols. For a comprehensive literature survey, we listed the analytical performances of various mouse IgG immunoassays in the upper part of Table 1. Comparing with all the immunoassay protocols based on the PEC method in spite of the different analytes, as displayed in the lower part of Table 1, this immunoassay still exhibited apparent superiority due to the synergy effect existing in this PEC immunoassay.

Reproducibility, Specificity, Stability, and Application in Real Sample. The precision and reproducibility of this PEC immunoassay was evaluated by within-batch (intra-assay) and a between-batch (interassay) relative standard deviation (RSD). Analyzed from the experimental results, the intra-assay RSD were 5.8%, 6.1%, and 6.6% at 0.1, 0.5, and 1.0 ng/mL, respectively, whereas the interassay RSD of 6.4%, 7.0%, and 7.5% were obtained by measuring the same samples with four electrodes prepared independently at the identical experimental conditions. These results suggested an acceptable precision and reproducibility of the proposed protocol.

Specificity is an essential criterion for immunoassay since the existing of the nonspecific adsorption. To reveal the selectivity of the binding, control experiments were performed. The photocurrent responses of the Ab_1 modified photoelectrodes to goat IgG, rabbit IgG, or human IgG at the same concentration of 0.1 ng/mL were shown in Figure 5. As can be seen, the

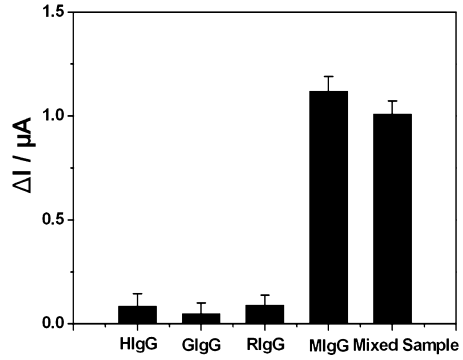

Figure 5. (A) Selectivity of the proposed immunoassay to mouse IgG (MIgG) by comparing it to the interfering proteins at the 0.1 ng/mL level: human IgG (HIgG), goat IgG (GIgG), rabbit IgG (RIgG), and the mixed-sample. The error bars showed the standard deviation of four replicate determinations.

photocurrent responses from goat IgG, rabbit IgG, or human IgG were much lower than that of mouse IgG, demonstrating that the photocurrent reduction is due to the specific binding. The specificity of the proposed immunoassay was also evaluated by measuring the responses of mouse IgG in the mixed sample composed of 0.1 ng/mL mouse IgG and goat IgG, rabbit IgG, and human IgG at the same concentration of 10 ng/mL. No significant difference of photocurrent response could be observed as compared to the result obtained in the presence of only mouse IgG at the concentration of 0.1 ng/mL. All these results implied that the proposed immunoassay had acceptable selectivity without obvious interference from nonspecific adsorption.

The stability of the immunoassay system was examined by performing the detection of 1.0 ng/mL Ag. After 15 repeated

dx.doi.org/10.1021/ac203184g | Anal. Chem. 2012, 84, 917−923

measurements, the photocurrent was unchanged over time, indicating the stable readout for signal collection. If the Ab_1-modified electrode was stored in PBS at 4 °C in darkness over 2 weeks, no apparent change in photocurrent response in the detection of same Ag concentration was found, demonstrating its good long-term storage stability.

The feasibility of the immunoassay system for clinical applications was investigated using several real samples of mouse serum. These serum samples were diluted to specific concentrations with a PBS of 7.4. The recoveries of 0.01, 0.1, 0.5, 1.0, and 5.0 ng/mL of mouse IgG were determined with the results shown in Table S-1 in the Supporting Information. The acceptable recoveries ranging from 89.3% to 112% indicated that it was feasible to utilize the developed immunoassay for practical applications.

CONCLUSIONS

In this study, we present an example of HRP stimulated BCP in QDs-based PEC immunoassay for enhanced amplification. As compared to the conventional label-free or GOx labeled PEC immunoassays with enhanced steric hindrances or donor concentration as the exclusive cause for signal variation, this new biosensing strategy possesses higher sensitivity by means of multi amplification via HRP-labeled Ab_2, not only enhancing the effect of steric hindrance greatly but also introducing the HRP competitive absorption and the BCP amplification route into the system that alter the light-absorption feature of the electrode. Since HRP or various enzymes which could stimulate the BCP of insoluble products may also be used as a label for the exploitation in different immunoreactions or other recognition events, the proposed detection format of amplified PEC immunoassay might open a new perspective for the development of a highly sensitive PEC detection system.

ASSOCIATED CONTENT

Supporting Information

Additional information as noted in text. This material is available free of charge via the Internet at http://pubs.acs.org.

AUTHOR INFORMATION

Corresponding Author

*Phone/fax: +86-25-83597294. E-mail: xujj@nju.edu.cn.

ACKNOWLEDGMENTS

This work was supported by the 973 Program (Grant 2012CB932600), the National Natural Science Foundation (Grants 21025522 and 21135003), and the National Natural Science Funds for Creative Research Groups (Grant 20821063).

REFERENCES

(1) Liu, X.; Dai, Q.; Austin, L.; Coutts, J.; Knowles, G.; Zou, J. H.; Chen, H.; Huo, Q. *J. Am. Chem. Soc.* **2008**, *130*, 2780.
(2) Schaefer, O.; Bohlmann, R.; Schleuning, W. D.; Schulze-Forster, K.; Hümpel, M. *J. Agric. Food Chem.* **2005**, *53*, 2881.
(3) Ocvirk, R.; Franklin, K. B. J.; Pearson Murphy., B. E. *Anal. Chem.* **2009**, *81*, 1191.
(4) Zuo, B. L.; Li, S. M.; Guo, Z.; Zhang, J. F.; Chen, C. Z. *Anal. Chem.* **2004**, *76*, 3536.
(5) Mayer, K. M.; Lee, S.; Liao, H. W.; Rostro, B. C.; Fuentes, A.; Scully, P. T.; Nehl, C. L.; Hafner, J. H. *ACS Nano* **2008**, *2*, 687.
(6) Tang, D. P.; Tang, J.; Su, B. L.; Chen, G. N. *J. Agric. Food Chem.* **2010**, *58*, 10824.
(7) Shan, Y.; Xu, J. J.; Chen, H. Y. *Chem. Commun.* **2010**, *46*, 5079.
(8) Ronkainen-Matsuno, N. J.; Thomas, J. H.; Halsall, H. B.; Heineman, W. R. *TrAC, Trends Anal. Chem.* **2002**, *21*, 213.
(9) Ronkainen, N. J.; Halsall, H. B.; Heineman, W. R. *Chem. Soc. Rev.* **2010**, *39*, 1747.
(10) Liang, M. M.; Liu, S. L.; Wei, M. Y.; Guo, L. H. *Anal. Chem.* **2006**, *78*, 621.
(11) Zhang, X. R.; Li, S. G.; Jin, X.; Zhang, S. S. *Chem. Commun.* **2011**, *47*, 4929.
(12) Zhang, X. R.; Zhao, Y. Q.; Li, S. G.; Zhang, S. S. *Chem. Commun.* **2010**, *46*, 9173.
(13) Zhu, W.; An, Y. R.; Luo, X. M.; Wang, F.; Zheng, J. H.; Tang, L. L.; Wang, Q. J.; Zhang, Z. H.; Zhang, W.; Jin, L. T. *Chem. Commun.* **2009**, *45*, 2682.
(14) Zhao, W. W.; Wang, J; Xu, J. J.; Chen, H. Y. *Chem. Commun.* **2011**, *47*, 10990.
(15) Zhao, W. W.; Tian, C. Y.; Xu, J. J.; Chen, H. Y. *Chem. Commun.* **2011**, *48*, 895−897.
(16) Wang, G. L.; Xu, J. J.; Chen, H. Y. *Biosens. Bioelectron.* **2009**, *24*, 2494.
(17) Qian, Z.; Bai, H. J.; Wang, G. L.; Xu, J. J.; Chen, H. Y. *Biosens. Bioelectron.* **2010**, *25*, 2045.
(18) Haddour, N.; Cosnier, S.; Gondran, C. *Chem. Commun.* **2004**, 2472.
(19) Haddour, N.; Chauvin, J.; Gondran, C.; Cosnier, S. *J. Am. Chem. Soc.* **2006**, *128*, 9693.
(20) Wang, G. L.; Xu, J. J.; Chen, H. Y.; Fu, S. Z. *Biosens. Bioelectron.* **2009**, *25*, 791.
(21) Wang, G. L.; Yu, P. P.; Xu, J. J.; Chen, H. Y. *J. Phys. Chem. C* **2009**, *113*, 11142.
(22) Kang, Q.; Yang, L. X.; Chen, Y. F.; Luo, S. L.; Wen, L. F.; Cai, Q. Y.; Yao., S. Z. *Anal. Chem.* **2010**, *82*, 9749.
(23) An, Y. R.; Tang, L. L.; Jiang, X. L.; Chen, H.; Yang, M. C.; Jin, L. T.; Zhang, S. P.; Wang, C. G.; Zhang, W. *Chem.—Eur. J.* **2010**, *16*, 14439.
(24) Patolsky, F.; Lichtenstein, A.; Willner, I. *Chem.—Eur. J.* **2003**, *9*, 1137.
(25) Sheng, Q. L.; Zheng, J. B. *Biosens. Bioelectron.* **2009**, *24*, 1621.
(26) Zhao, W. W.; Yu, P. P.; Xu, J. J.; Chen, H. Y. *Electrochem. Commun.* **2011**, *13*, 495.
(27) Gill, R.; Zayats, M.; Willner, I. *Angew. Chem., Int. Ed.* **2008**, *47*, 7602.
(28) Lao, U. L.; Mulchandani, A.; Chen, W. *J. Am. Chem. Soc.* **2006**, *128*, 14756.
(29) Dong, X. Y.; Mi, X. N.; Zhao, W. W.; Xu, J. J.; Chen, H. Y. *Biosens. Bioelectron.* **2011**, *26*, 3654.
(30) Wang, J.; Shan, Y.; Zhao, W. W.; Xu, J. J.; Chen, H. Y. *Anal. Chem.* **2011**, *83*, 4004.
(31) Yissar, V. P.; Katz, E.; Wasserman, J.; Willner, I. *J. Am. Chem. Soc.* **2003**, *125*, 622.
(32) Cui, R. J.; Pan, H. C.; Zhu, J. J.; Chen, H. Y. *Anal. Chem.* **2007**, *79*, 8494.
(33) Tang, D. P.; Su, B. L.; Tang, J.; Ren, J. J.; Chen, G. N. *Anal. Chem.* **2010**, *82*, 1527.
(34) Chen, D.; Zhang, H.; Li, X.; Li, J. H. *Anal. Chem.* **2010**, *82*, 2253.
(35) http://www.alpco.com/products/IgG_Mouse_ELISA.asp.
(36) Lai, G. S.; Yan, F.; Wu, J.; Leng, C.; Ju, H. X. *Anal. Chem.* **2011**, *83*, 2726.
(37) Chan, C. P. Y; Bruemmel, Y.; Seydack, M.; Sin, K. K.; Wong, L. W.; Merisko-Liversidge, E.; Trau, D.; Renneberg, R. *Anal. Chem.* **2004**, *76*, 3638.
(38) Deng, J. J.; Song, Y.; Wang, Y.; Di, J. W. *Biosens. Bioelectron.* **2010**, *26*, 615.
(39) Sakharov, I. Y.; Alpeeva, I. S.; Efremov, E. E. *J. Agric. Food Chem.* **2006**, *54*, 1584.